Retardation-induced phase singularities in coupled plasmonic oscillators

Sven M. Hein[1,2,*] and Harald Giessen[2,†]

[1]*Institut für Theoretische Physik, Nichtlineare Optik und Quantenelektronik, Technische Universität Berlin, Hardenbergstraße 36, 10623 Berlin, Germany*

[2]*4th Physics Institute and Research Center SCoPE, Universität Stuttgart, Pfaffenwaldring 57, 70550 Stuttgart, Germany*

(Received 15 December 2014; revised manuscript received 22 April 2015; published 7 May 2015)

We show that two coupled, stacked plasmonic scatterers exhibit surprisingly complex excitation spectra as soon as retardation plays a role in the coupling. At a certain stacking distance and a certain frequency, the amplitude and phase exhibit sharp features, and the phase difference between the scatterers shows a singularity, which constitutes a vortex. Above this singularity, the antisymmetric oscillation that arises from plasmon hybridization ceases to exist and is replaced by a second, *symmetric* oscillation. We examine the distance-dependent behavior of these phenomena by an analytical coupled-dipole model as well as by numerical simulations of stacked split-ring resonators and show that the singularity can be explained as an antiresonance. Furthermore, we present a simple necessary and sufficient condition under which the oscillations have a phase difference of exactly zero or π in case of arbitrary retardation and therefore exhibit the intrinsic symmetry of the system. We show that this condition implies that the spectral positions of (anti)symmetric oscillations do not coincide with the spectral positions of the (anti)symmetric mode. The vortices that are present at the phase singularities might be used to generate light with angular optical momentum in plasmonic metasurfaces.

DOI: 10.1103/PhysRevB.91.205402 PACS number(s): 78.67.Pt, 78.20.Bh, 73.20.Mf

I. INTRODUCTION

In recent years, vertically stacked plasmonic nanostructures have gained much attention since they allow for truly three-dimensional metamaterials [1–8], plasmonic rulers [9,10], and nanoantennas [11]. Due to the coupling of the single constituents, the spectra of these nanostructures show complex features, such as multiple peaks or Fano resonances [12–17]. In many cases, the behavior has been successfully described by the plasmon hybridization model, introduced by Nordlander *et al.* [18]. As long as the coupling is near-field mediated, the finite value of the speed of light can be neglected and the interaction can be seen as instantaneous. For chains or arrays of nanoparticles, however, retardation is needed to describe the behavior of these extended structures [19,20]. Only recently, the effects of retardation in single-particle coupling have moved into the focus of scientific research [21–23]. For linear processes, retardation can be formulated as a complex frequency-dependent coupling constant, derived from the dyadic Green's tensor that connects the polarization of one nanoparticle to the field at the position of the other nanoparticle [24]. Retardation can produce effects similar to electromagnetically induced absorption [25,26] or create sharp resonances [27].

In order to use this additional degree of freedom, we have to understand the implications of a complex coupling constant on the excitation spectrum. Therefore, we study the most fundamental realization of a retardedly coupled system, i.e., two coupled dipoles (see Fig. 1). In case of near-field coupling, we expect a symmetric and an antisymmetric oscillation at two different resonance frequencies due to plasmon hybridization [18,28], while in the limit of large distances coupling should be negligible and the two scatterers should behave like two uncoupled oscillators. In between these two regions, the mutual coupling and the coupling to the external field are of similar strength. The coherent superposition of these two coupling effects leads to exciting phenomena, such as vortexlike phase singularities and the transformation of an antisymmetric to a symmetric oscillation [Fig. 1(b)], which we will discuss in this paper. These singularities appear when the external excitation and the near field of one oscillator perfectly annihilate at the position of the other oscillator due to destructive interference. Around such so-called antiresonances one finds a strong frequency dependence of oscillator amplitude and phase.

Our model system has strong similarities with the one studied by Fischer and Martin [21], which showed periodic intensity fluctuations of the plasmon resonance when the nanoparticle distance is varied. In our paper, however, we focus on the phase of two retardedly coupled nanostructures which shows a very complex behavior down to stacking distances of less than $1/10$ of a wavelength.

II. ANALYTICAL MODEL

An intuitive way to describe plasmonic resonances is a driven harmonic oscillator. If we describe the charge distribution in the nanostructure by its electric dipole moment $\boldsymbol{p}$, which is driven by an external electric field $\boldsymbol{E}^{\mathrm{ext}}$, and also include radiation damping [29], this leads to

$$\boldsymbol{p} = \alpha \boldsymbol{E}^{\mathrm{ext}} \tag{1}$$

with the polarizability

$$\alpha = \frac{A}{\omega_0^2 - i\gamma\omega - \omega^2 - 2iA\omega^3/(3c^3)}. \tag{2}$$

A denotes the strength of the plasmonic resonance, ω_0 denotes its (angular) resonance frequency, and γ includes all nonradiative losses. We would like to point out that the

*shein@itp.tu-berlin.de

†h.giessen@pi4.uni-stuttgart.de

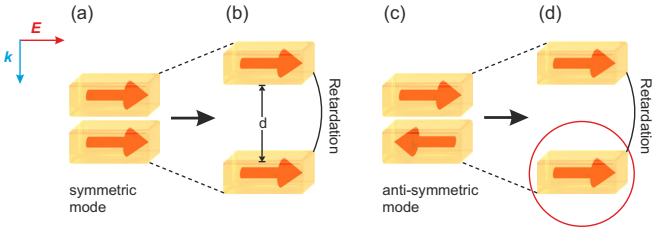

FIG. 1. (Color online) Closely stacked dipolar plasmonic oscillators show two resonances with a phase difference of zero and π [(a) and (c)]. By increasing the stacking distance d [(b) and (d)], retardation is introduced which substantially changes the phase of the coupling as well as of the exciting electric field. This can lead to the transformation of the antisymmetric oscillation into a symmetric oscillation (d).

resulting radiatively damped harmonic oscillator spectrum has strong similarities, but is not equal to a Lorentzian spectrum.

In the case of two coupled plasmonic oscillators $\boldsymbol{p}_1$ and $\boldsymbol{p}_2$, both are excited not only by the external electric field but also by the electric field of the other oscillator, which can be calculated via the dyadic Green's function G_{ij}:

$$\boldsymbol{p}_i = \alpha_i\left(\boldsymbol{E}_i^{\text{ext}} + G_{ij}\boldsymbol{p}_j\right), \tag{3}$$

where α_i denotes the polarizability of the respective dipole. For simplification, we assume the scatterers to be similar, i.e., that they react equally to the exciting field: $\alpha_1 = \alpha_2 \overset{\text{def}}{=} \alpha$. We also let the interaction be symmetric, i.e., $G_{ij} = G_{ji} \overset{\text{def}}{=} G$. For plasmonic resonances, the orientation of the dipole moment is often given by the shape of the particle. Therefore, we can describe the polarization by a single complex *scalar* p_i, and we do not need to care about its orientation. This also makes G_{ij} scalar. For more complex plasmonic resonances, a whole coupling tensor [30] might be needed. However, for many common shapes, the approximation of the plasmon resonance by a dipole is very good and quite common, which is why we stick to the dipole picture. At the end of this publication, we demonstrate numerical simulations of more complex nanostructures, namely, split-ring resonators, and find that the discussed effects are also present. Using Eq. (3), it is easy to show that the polarizations are given by

$$\begin{pmatrix} p_1 \\ p_2 \end{pmatrix} = \frac{\alpha}{1-(\alpha G)^2}\begin{pmatrix} 1 & \alpha G \\ \alpha G & 1 \end{pmatrix}\begin{pmatrix} E_1^{\text{ext}} \\ E_2^{\text{ext}} \end{pmatrix}. \tag{4}$$

From the matrix elements in Eq. (4) we can deduce that $|\alpha G|$ is a measure for the energy transfer between the structures. For $|\alpha G| < 1$, each oscillator is mainly excited by the external field at its own position, and the coupling to the other dipole can be regarded as a perturbation. In this regime, we can understand the prefactor $\frac{1}{1-(\alpha G)^2}$ as the result of the Born series $1 + (\alpha G)^2 + (\alpha G)^4 + \cdots$ which takes care of all scattering processes. For $|\alpha G| > 1$, however, the external field at the position of the *other* dipole gives the largest contribution to the polarization. In this case, the Born series above no longer converges and we have reached the region of "strong energy exchange," in which the mutual interaction cannot be described as a perturbation. For the exact value $\alpha G = \pm 1$, Eq. (4) is not well defined since the denominator becomes zero. However, since polarizations need to be finite for finite distances between the nanostructure and finite external excitation, the limit of $p_{1,2}$ for $\alpha G \to \pm 1$ will exist for all physical situations.

If one diagonalizes the polarizability matrix in Eq. (4) that relates the polarizations to the external fields, the *modes* of the system can be recovered. For symmetry reasons [18], there exists a symmetric and an antisymmetric mode regardless of the coupling distance. The symmetric (antisymmetric) mode will be the only excited mode if $E_1^{\text{ext}} = E_2^{\text{ext}}$ (if $E_1^{\text{ext}} = -E_2^{\text{ext}}$). It is important to differentiate between *modes* and *oscillations*: Modes are properties of the coupled system, independent of the excitation, which show the aforementioned symmetry properties in their phase. What is, however, visible in an experiment will be the actual dynamics of the two driven oscillators, which will generally be a coherent superposition of the two modes, with an amplitude and relative phase depending on the external field. This coherent superposition will lead to the complex phase behavior seen in our simulations. With Eqs. (2) and (4) the polarizabilities of the two hybridized symmetric and antisymmetric modes are given by

$$\alpha_{\substack{\text{s}\\\text{a}}} = \frac{A}{\omega_0^2 - i\gamma\omega - \omega^2 - 2iA\omega^3/(3c^3) \mp AG}, \tag{5}$$

which shows that AG determines the frequency shift as well as spectral broadening (bright mode) or narrowing (dark mode). This quantity, and not αG, is usually referred to as the "coupling strength." However, as we will show now, it is αG that determines the phase between two coupled plasmonic oscillators.

Therefore we investigate the behavior of two vertically stacked dipoles that are excited with plane waves along their stacking direction z (see Fig. 1). The Green's function is then given by

$$G = \frac{\exp(ikz)}{z^3}[(kz)^2 + ikz - 1] \tag{6}$$

and the external plane-wave excitation is $E \cdot \binom{1}{e^{ikz}}$. To calculate α, we used the values given in Table I. First, we examine the phase difference of the oscillators to the external field (see Fig. 2), given as $\phi_{1,2} = \arg(\frac{p_{1,2}}{E_{1,2}^{\text{ext}}})$. In case of the oscillator being excited first [Fig. 2(a)], the phase lag increases smoothly from zero at low frequencies to π at high frequencies and does not show strong qualitative differences at different stacking distances. In Fig. 2(b), we explicitly plot the phase of p_1 for stacking distances of 100 nm (red, solid line) and 150 nm (blue, dashed line). For the 100-nm case, we observe a zero crossing slightly above 150 THz, which, however, only seems like a strong feature due to our choice [31] to plot the phase between -2π and zero. More importantly, we find a two-step behavior of the phase, which is not present at a stacking distance of 150 nm.

However, the phase of the oscillator excited second shows a qualitatively different behavior for stacking distances below

TABLE I. Values used to model the polarizability α.

ω_0	$2\pi \times 200\,\text{THz}$
γ	125 THz
A	$400\,000\,\text{nm}^3 \times \omega_0^2$

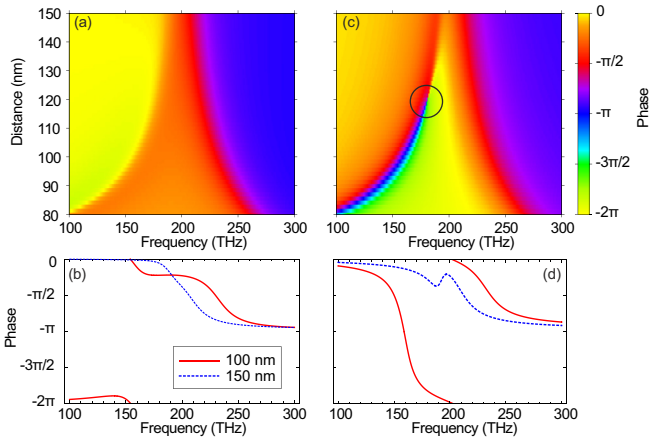

FIG. 2. (Color online) Phase between the oscillating dipole and external field, depending on the stacking distance. (a,b) Oscillator excited first. (c,d) Oscillator excited second. In case (a) the phase lag goes from zero to π without any strong phase changes for any coupling distance. In (b) we show the phase of the first oscillator at two distinct stacking distances, 100 nm (red, solid line) and 150 nm (blue, dashed line). The phase has negative values, since the oscillator is *lagging behind* the external excitation. The apparent "jump" of the red curve slightly above 150 THz is only a zero crossing of the phase. We discover a "two-step" behavior for the 100-nm case. For the second dipole (c,d) the situations differ strongly for between stacking distances below and above 120 nm. Below 120 nm, the phase lag takes every possible value from zero up to 2π at the low-frequency branch until it finally goes to π at high frequencies, while at higher distances the phase lag only changes to a value below π, then goes back to zero, until it goes up to π. We see this behavior also in (d), where again the phase at 100 nm (red, solid line) and 150 nm (blue, dashed line) is shown. The transition point exhibits a singularity in the phase, marked by the black circle.

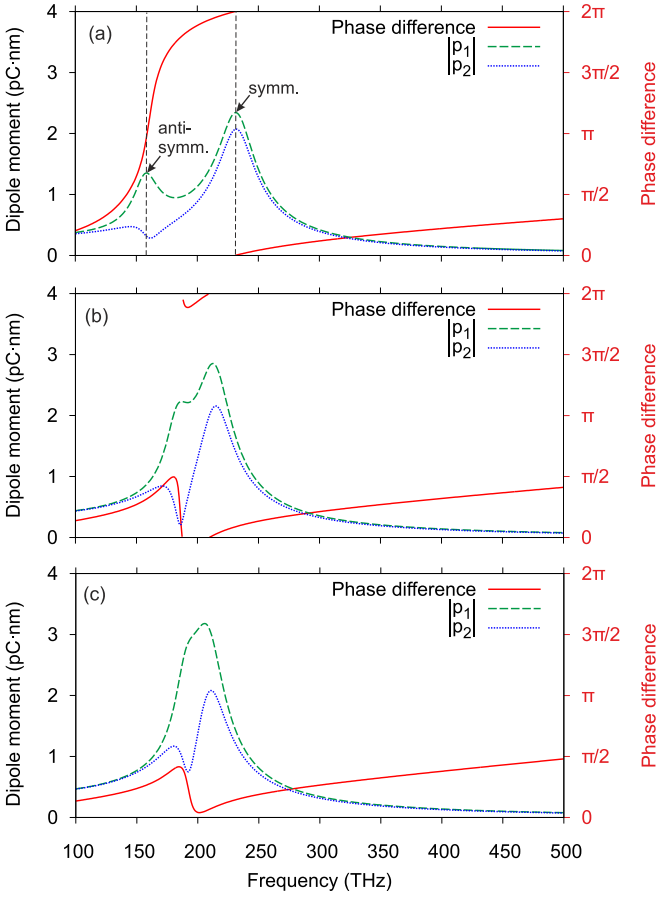

FIG. 3. (Color online) Absolute values of polarizations p_1 (green, dashed) and p_2 (blue, dotted) and their phase difference (red, solid, labels at right axis) at different stacking distances: (a) 100 nm, (b) 130 nm, and (c) 150 nm. For 100 nm, the two modes are clearly separated. The first oscillator has a spectrum consisting of two overlapping Lorentzian peaks, where the phase difference at the first peak is π (antisymmetric mode), while it is zero at the second peak (symmetric mode). The second oscillator has a more complex line shape. The two modes are marked by the dashed lines. For 130 nm, which is just above the phase singularity, the phase difference does not reach π anymore; instead, it crosses the zero line twice. While $|p_1|$ still has the shape of two Lorentzians, $|p_2|$ shows a sharp dip. For 150 nm, the phase shows only a slight modulation around the resonance, reaching neither zero nor π. While the two resonances are barely distinguishable in $|p_1|$, the sharp dip in $|p_2|$ is still visible, leading to two distinct peaks.

and above 120 nm. At 120 nm, the phase exhibits a vortexlike singularity at about 180 THz [see Fig. 2(c)]. Below this vortex, the phase starts at zero at low frequencies as well, but then reaches every possible value until it reaches zero again and finally becomes π at high frequencies. For stacking distances above the vortex, this complex behavior is replaced by a phase that changes from zero to a value smaller than π, then decreases back to zero and finally reaches π. In Fig. 2(d) we plot the phase for the explicit stacking distances of 100 nm (red, solid line) and 150 nm (blue, dashed line), where we can also observe the qualitatively different behavior below and above the vortex.

At the singularity, the phase is not well defined, which implies that the polarization has to be zero at this point. Using Eq. (4) and setting $p_2 = 0$, we can deduce that this singularity appears for

$$\alpha G = -\exp(ikz). \tag{7}$$

In this case, the external excitation and the scattered field from the first dipole exactly cancel at the location of the second dipole and we are at the border between strong ($|\alpha G| > 1$) and weak energy transfer ($|\alpha G| < 1$). To gain a better understanding of the behavior around this special point, we calculate the amplitudes $|p_1|$ and $|p_2|$ of the two oscillations at stacking distances of 100 nm (below the vortex), 130 nm (slightly above the vortex), and 150 nm (highly above the vortex). We also analyze the phase *difference* between the two oscillators, defined as $\Delta\phi = \arg(\frac{p_1}{p_2})$. The results are depicted in Fig. 3. At 100 nm distance, $|p_1|$ shows two clear peaks, at which the phase difference is either π (antisymmetric mode) or zero (symmetric mode), demonstrating the validity of the plasmon hybridization picture. The behavior of $|p_2|$ is more complex, with asymmetric features especially at the antisymmetric mode. We see that although plasmon hybridization gives two modes with a damped harmonic oscillator line shape each, the behavior of the second oscillator cannot be described by a simple double-peak spectrum. This is of course due to the fact that we always excite a coherent superposition of the two modes, but it can also be understood as the second dipole "lying

in the shadow" of the first one, which intuitively explains why the spectrum of $|p_1|$ closely resembles a double-Lorentzian spectrum, while p_2 does not.

At 130 nm distance [Fig. 3(b)], the phase difference does not reach π, but crosses the zero line *twice*. This is remarkable because it seems to contradict plasmon hybridization. Due to symmetry reasons, however, the two *eigenmodes* of the system are always symmetric and antisymmetric. Nevertheless, in this configuration there exists no frequency at which a perfectly antisymmetric oscillation is excited. The appearance of the second zero crossing will be explained below where we derive a condition for perfectly (anti)symmetric oscillations. The amplitude $|p_1|$ still shows two overlapping peaks, while $|p_2|$ shows a strong dip. This dip reaches zero at the vortex and the frequency dependence of $|p_2|$ becomes nondifferentiable. However, qualitatively the frequency dependence of $|p_{1,2}|$ does not differ much between the plotted case of 130-nm distance and the exact distance at which the vortex occurs.

Finally, at $d = 150$ nm distance, the phase difference reaches neither zero nor π. In $|p_1|$ the two modes are barely distinguishable while in $|p_2|$ the strong dip is still visible [see Fig. 2(c)]. We can therefore distinguish three regimes: For strong interaction in the near field, there exists a symmetric as well as an antisymmetric oscillation. For weaker coupling and larger retardation, the antisymmetric oscillation ceases to exist and gives rise to a second, *symmetric* oscillation. Eventually, both of these symmetric oscillations disappear above a certain distance.

All this behavior is typical for the appearance of an *antiresonance* [32–34] of the second oscillator: Antiresonances appear when two different drivings of an oscillator interfere destructively in a way that the oscillator is not excited at all. In our case, these two drivings are the external field and the field scattered by the first oscillator. At an antiresonance, strong phase jumps occur such as the vortex seen in our system, and the two drivings "exchange roles." This role change is due to the fact that while the external driving maintains its intensity for different stacking distances the field from the first oscillator is strongly distance dependent. Although this happens at distances well below the wavelength, retardation is still crucial for the vortex to appear, since the symmetry in the driving of the two oscillators needs to be broken. In our case, this happens due to the different driving phase. Without retardation, both oscillators would always oscillate in phase and no vortex would be present. If the symmetry, however, is already broken, e.g., by coupling to different plasmonic scatterers, retardation is not required for antiresonances to appear. This is, for example, the case in planar dolmen structures [12] and other planar structures with Fano resonances [35].

III. CONDITIONS FOR (ANTI)SYMMETRIC OSCILLATIONS

If the two oscillators oscillate (anti)symmetrically, their phase difference $\Delta\phi = \arg(\frac{p_1}{p_2})$ is an even (odd) multiple of π. For nonvanishing $p_{1,2}$, in the symmetric as well as in the antisymmetric case, this is fulfilled if and only if

$$\mathrm{Im}\left(\frac{p_1}{p_2}\right) = 0. \tag{8}$$

We do not restrict ourselves to any angle of incidence for the external plane-wave excitation, and are therefore allowed to set the exciting field component to

$$\begin{pmatrix} E_1^{\mathrm{ext}} \\ E_2^{\mathrm{ext}} \end{pmatrix} = \begin{pmatrix} 1 \\ e^{i\phi} \end{pmatrix}. \tag{9}$$

Please note that due to our approximation mentioned in the beginning, namely, that the plasmonic resonance of each particle is only excited by one electric-field component—specifically the one pointing along its dipole moment—this ansatz is valid for both s- and p-polarized excitation. The only requirement which Eq. (9) states is that this component of the external excitation is of the same amplitude at the location of both nanostructures. Using Eqs. (4) and (8), we get

$$\begin{aligned} \mathrm{Im}\left(\frac{p_1}{p_2}\right) &= \mathrm{Im}\left(\frac{1+\alpha G e^{i\phi}}{\alpha G + e^{i\phi}}\right) \\ &= \frac{1}{|\alpha G + e^{i\phi}|^2}(|\alpha G|^2 - 1)\sin\phi \\ &\overset{\text{Eq.(8)}}{=} 0. \end{aligned} \tag{10}$$

This can only be fulfilled if either $\sin\phi = 0$, which means that we obey the Bragg condition and only excite one of the two modes, or

$$|\alpha G| = 1. \tag{11}$$

While the Bragg condition is fulfilled only for certain angles of incidence, Eq. (11) is independent of the angle of incidence and only depends on internal parameters such as the stacking distance and the polarizability. Therefore we can state that if and only if $|\alpha G| = 1$ the system will oscillate either symmetrically or antisymmetrically for arbitrary plane-wave excitation. This statement is not in conflict with the root appearing in the denominator of Eq. (4) for $\alpha G = \pm 1$: First of all, these roots appear only for exactly these two values, while the condition $|\alpha G| = 1$ is much more general. Second, for the

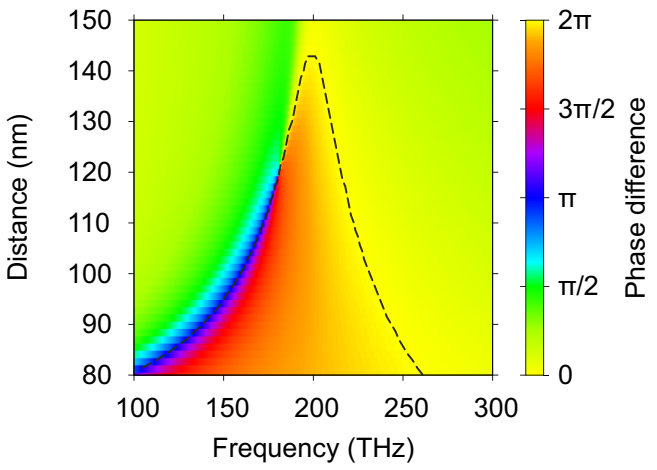

FIG. 4. (Color online) Phase difference between oscillators. Again we notice the phase singularity at 120 nm and 180 THz. The black dashed line marks the values with $|\alpha G| = 1$. Below the line, the energy transfer is strong, i.e., $|\alpha G| > 1$. At exactly $|\alpha G| = 1$, the phase difference is either zero or π. At the phase singularity, the π phase disappears and gets replaced by a second symmetric oscillation.

system to be physical, the limit $\alpha G \to \pm 1$ of all quantities must exist. This is one of the main results of this paper. It also shows that the frequencies of (anti)symmetric oscillations do not have to coincide with the spectral position of the pure (anti)symmetric modes; in fact, except for special cases like Bragg scattering, they differ.

Figure 4 shows the phase difference for different stacking heights and frequencies. The dashed line marks the points at which Eq. (11) is fulfilled. As shown, these points coincide with (anti)symmetric oscillations. Above the vortex, this condition is still met at two points in frequency space; however, then the overlap between the two modes is large enough that the symmetric oscillation can impose its behavior on both frequencies, which leads to two symmetric oscillations.

IV. NUMERICAL SIMULATIONS

To demonstrate that this complex behavior is not specific to single dipoles but also appears at more complex plasmonic scatterers, we simulated two stacked split-ring resonators (SRRs), a so-called stereometamaterial [36], using the commercially available finite element method solver CST Microwave Studio. SRRs couple through their electric as well as magnetic dipole moment [36–38] where the respective coupling strengths can be tuned by rotating one of the SRRs around the central axis [36]. The dimensions of the simulated SRRs can be found in Fig. 5(a). Gold was modeled using data from Johnson and Christy [39]. The structures are placed in vacuum. We analyzed the phase of the plasmonic resonance by reading out the electric field at a point in the gap which is centered in the SRR in the x and z direction and displaced 70 nm from the center in the y direction and by subtracting the field from the external plane-wave excitation.

As shown in Fig. 5(b), the phase singularity appears at $s = 95$ nm and $\nu = 198$ THz, however not as pronounced as in the point dipole case. Therefore, we infer that it is a common feature of coupled plasmonic systems and that the exact expression for G is not important. We would like to note that 95 nm is well within the range of experimental feasibility [2] and that one has to be very careful in describing the observed phenomena in terms of symmetric and antisymmetric oscillations, since one can easily reach stacking distances in which no antisymmetric oscillation occurs.

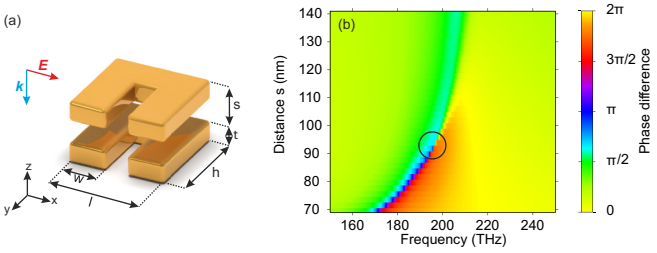

FIG. 5. (Color online) (a) Dimensions of the coupled SRRs used in the simulation: $l = h = 230$ nm, $w = 90$ nm, and $t = 50$ nm. s is varied in the simulation. (b) Phase difference between the oscillations of the upper and lower SRR. We see the appearance of the phase vortex at $s = 95$ nm and $\nu = 198$ THz (black circle), however not as pronounced as in the point dipole case.

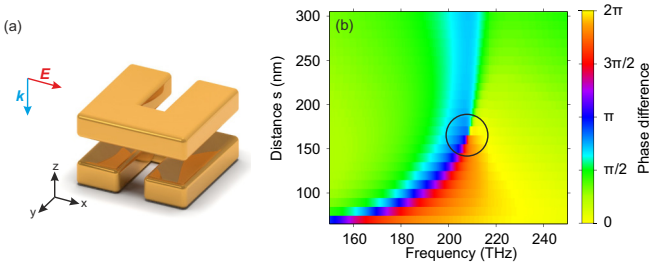

FIG. 6. (Color online) (a) The interaction can be enhanced by twisting one of the SRRs by 180 deg. (b) Phase difference between the oscillations of the upper and lower SRR. We see the appearance of the phase vortex at $s = 165$ nm and $\nu = 210$ THz. The effect is much more pronounced than in the nontwisted case.

We can enhance the effect by twisting the upper SRR by 180 deg around the central axis [Fig. 6(a)]. This retains the required symmetry, i.e., equal interaction with the external excitation, but causes electric and magnetic dipole coupling to add up constructively. Figure 6(b) demonstrates that the vortex is much more pronounced and the disappearance of the antisymmetric oscillation (blue) is clearly visible.

V. CONCLUSION

We have shown that plasmonic scatterers behave qualitatively differently at different stacking distances. In particular, a phase singularity appears at a certain frequency, which can be interpreted as an antiresonance. As any singularity yields a very sharp feature by definition, this might be useful for future sensing devices that directly probe the phase of one of the scatterers. Also, the strong frequency dependence of the *amplitude* of the second oscillator around the antiresonance could be used for local frequency-sensitive measurements, in analogy to current applications of Fano resonances [40]. By giving a simple necessary and sufficient condition for (anti)symmetric oscillations, we were able to explain the appearance of a second symmetric oscillation above the phase singularity. Since this condition holds for arbitrary angles of incidence, it follows that as soon as the oscillation is (anti)symmetric for one angle of incidence (that does not fulfill the Bragg condition) it is (anti)symmetric for *any* angle of incidence.

Coupled harmonic oscillators have been one of the most fundamental building blocks of physical theories for centuries, since their behavior is easy to understand. Therefore in our opinion the richness of features that occur as soon as retardation is introduced is remarkable and makes retardation one of the most interesting degrees of freedom for tuning the response of coupled plasmonic oscillators. In the future, the vortices that are present at the phase singularities might be used to generate light with optical angular momentum in plasmonic metasurfaces when combining the coupled plasmonic systems with appropriate lateral and spatial design.

ACKNOWLEDGMENTS

We would like to thank the European Research Council (ComplexPlas), the Deutsche Forschungsgemeinschaft (DFG), the Bundesministerium für Bildung und Forschung, the

Baden-Württemberg Stiftung, the Alexander-von-Humboldt-Stiftung, the German Israeli Foundation, and the Carl-Zeiss-Stiftung for support. S.M.H. also acknowledges funding by the Deutsche Forschungsgemeinschaft through the Collaborative Research Centers SFB 910 and SFB 787 (School of Nanophotonics).

[1] C. Rockstuhl, F. Lederer, C. Etrich, T. Pertsch, and T. Scharf, Phys. Rev. Lett. **99**, 017401 (2007).
[2] N. Liu, H. Guo, L. Fu, S. Kaiser, H. Schweizer, and H. Giessen, Nat. Mater. **7**, 31 (2008).
[3] J. Valentine, S. Zhang, T. Zentgraf, E. Ulin-Avila, D. A. Genov, G. Bartal, and X. Zhang, Nature (London) **455**, 376 (2008).
[4] M. Decker, R. Zhao, C. M. Soukoulis, S. Linden, and M. Wegener, Opt. Lett. **35**, 1593 (2010).
[5] C. M. Soukoulis and M. Wegener, Nat. Photon. **5**, 523 (2011).
[6] C. Helgert, E. Pshenay-Severin, M. Falkner, C. Menzel, C. Rockstuhl, E.-B. Kley, A. Tünnermann, F. Lederer, and T. Pertsch, Nano Lett. **11**, 4400 (2011).
[7] B. Kanté, Y.-S. Park, K. O'Brien, D. Shuldman, N. D. Lanzillotti-Kimura, Z. Jing Wong, X. Yin, and X. Zhang, Nat. Commun. **3**, 1180 (2012).
[8] H. Moser and C. Rockstuhl, Laser Photon. Rev. **6**, 219 (2012).
[9] N. Liu, M. Hentschel, T. Weiss, A. P. Alivisatos, and H. Giessen, Science **332**, 1407 (2011).
[10] T. J. Davis, M. Hentschel, N. Liu, and H. Giessen, ACS Nano **6**, 1291 (2012).
[11] D. Dregely, R. Taubert, J. Dorfmüller, R. Vogelgesang, K. Kern, and H. Giessen, Nat. Commun. **2**, 267 (2011).
[12] B. Gallinet and O. J. F. Martin, Phys. Rev. B **83**, 235427 (2011).
[13] B. Gallinet and O. J. F. Martin, Opt. Express **19**, 22167 (2011).
[14] M. Frimmer, T. Coenen, and A. F. Koenderink, Phys. Rev. Lett. **108**, 077404 (2012).
[15] J. B. Lassiter, H. Sobhani, J. A. Fan, J. Kundu, F. Capasso, P. Nordlander, and N. J. Halas, Nano Lett. **10**, 3184 (2010).
[16] N. Verellen, Y. Sonnefraud, H. Sobhani, F. Hao, V. V. Moshchalkov, P. V. Dorpe, P. Nordlander, and S. A. Maier, Nano Lett. **9**, 1663 (2009).
[17] N. Feth, M. König, M. Husnik, K. Stannigel, J. Niegemann, K. Busch, M. Wegener, and S. Linden, Opt. Express **18**, 6545 (2010).
[18] P. Nordlander, C. Oubre, E. Prodan, K. Li, and M. I. Stockman, Nano Lett. **4**, 899 (2004).
[19] R. de Waele, A. F. Koenderink, and A. Polman, Nano Lett. **7**, 2004 (2007).
[20] M. Decker, N. Feth, C. M. Soukoulis, S. Linden, and M. Wegener, Phys. Rev. B **84**, 085416 (2011).
[21] H. Fischer and O. J. F. Martin, Opt. Lett. **34**, 368 (2009).
[22] R. Taubert, R. Ameling, T. Weiss, A. Christ, and H. Giessen, Nano Lett. **11**, 4421 (2011).
[23] P. Lunnemann, I. Sersic, and A. F. Koenderink, Phys. Rev. B **88**, 245109 (2013).
[24] F. Scheck, *Classical Field Theory* (Springer, Berlin, 2012).
[25] R. Taubert, M. Hentschel, J. Kästel, and H. Giessen, Nano Lett. **12**, 1367 (2012).
[26] P. Tassin, L. Zhang, R. Zhao, A. Jain, T. Koschny, and C. M. Soukoulis, Phys. Rev. Lett. **109**, 187401 (2012).
[27] S. Zhang, Z. Ye, Y. Wang, Y. Park, G. Bartal, M. Mrejen, X. Yin, and X. Zhang, Phys. Rev. Lett. **109**, 193902 (2012).
[28] F. von Cube, S. Irsen, R. Diehl, J. Niegemann, K. Busch, and S. Linden, Nano Lett. **13**, 703 (2013).
[29] I. Sersic, C. Tuambilangana, T. Kampfrath, and A. F. Koenderink, Phys. Rev. B **83**, 245102 (2011).
[30] F. B. Arango and A. F. Koenderink, New J. Phys. **15**, 073023 (2013).
[31] We chose negative values for the phase since the oscillator should always react on the external field and therefore lag behind it. This is in some way an arbitrary choice, though, since the function is 2π periodic, and often other plot ranges such as $(-\pi,\pi)$ are found in the literature.
[32] T. Koschny, P. Markoš, D. R. Smith, and C. M. Soukoulis, Phys. Rev. E **68**, 065602 (2003).
[33] C. Sames, H. Chibani, C. Hamsen, P. A. Altin, T. Wilk, and G. Rempe, Phys. Rev. Lett. **112**, 043601 (2014).
[34] D. Maystre, A.-L. Fehrembach, and E. Popov, J. Opt. Soc. Am. A **28**, 342 (2011).
[35] B. Luk'yanchuk, N. I. Zheludev, S. A. Maier, N. J. Halas, P. Nordlander, H. Giessen, and C. T. Chong, Nat. Mater. **9**, 707 (2010).
[36] N. Liu, H. Liu, S. Zhu, and H. Giessen, Nat. Photon. **3**, 157 (2009).
[37] H. Liu, J. X. Cao, S. N. Zhu, N. Liu, R. Ameling, and H. Giessen, Phys. Rev. B **81**, 241403 (2010).
[38] D. A. Powell, K. Hannam, I. V. Shadrivov, and Y. S. Kivshar, Phys. Rev. B **83**, 235420 (2011).
[39] P. B. Johnson and R. W. Christy, Phys. Rev. B **6**, 4370 (1972).
[40] B. Gallinet and O. J. F. Martin, ACS Nano **7**, 6978 (2013).